Antiwindup Controllers for Systems with Input Nonlinearities

Wassim M. Haddad* and Vikram Kapila†
Georgia Institute of Technology, Atlanta, Georgia 30332-0150

I. Introduction

IN practical real world applications the control-system design process must account for plant input nonlinearities arising from control actuation devices that are subject to amplitude saturation. These input nonlinearities can severely degrade the closed-loop system performance and in some cases drive the system to instability. Traditionally, the input saturation problem is treated by ad hoc desensitization schemes that are based on designer intuition with no a priori guarantees of system stability and performance. A recent resurgence of interest in this area has led to multivariable design techniques that a priori account for saturation nonlinearities.[1–3]

In a recent paper[3] a framework for designing fixed-architecture dynamic output feedback controllers for systems with input-output time-varying nonlinearities was developed. In particular, the framework in Ref. 3 is based on the classical Luré problem concerning the stability of a feedback loop involving sector-bounded nonlinearities. In the present Note, we use the framework presented in Ref. 3 to develop a synthesis algorithm to address the control saturation problem. Specifically, a homotopy continuation algorithm is presented and then applied to several benchmark problems.

II. Absolute Stabilization for Systems with Input Nonlinearities

In this section we introduce the absolute stabilization problem. The goal of the problem is to determine a linear time-invariant dynamic output feedback compensator that stabilizes a given linear dynamic system with input nonlinearities $\phi(u) \in \Phi$.

Absolute Stabilization Problem. Given the nth-order stabilizable and detectable plant with input nonlinearities $\phi(u) \in \Phi$,

$$\dot{x}(t) = Ax(t) - B\phi[u(t)], \qquad x(0) = x_0, \qquad t \geq 0 \tag{1}$$

$$y(t) = Cx(t) \tag{2}$$

where $x(t) \in \mathbb{R}^n$, $u(t) \in \mathbb{R}^m$, and $y(t) \in \mathbb{R}^l$, determine an n_cth-order linear time-invariant dynamic compensator

$$\dot{x}_c(t) = A_c x_c(t) + B_c y(t), \qquad x_c(0) = x_{c0} \tag{3}$$

$$u(t) = C_c x_c(t) \tag{4}$$

such that the closed-loop system (1–4) is asymptotically stable for all $\phi(u) \in \Phi$.

To characterize the class Φ of time-invariant sector bounded memoryless nonlinearities, the following definitions are needed. Let $M_1, M_2 \in \mathbb{R}^{m\times m}$ be given diagonal matrices such that $M_1 = \mathrm{diag}(M_{1_1}, \ldots, M_{1_m})$, $M_2 = \mathrm{diag}(M_{2_1}, \ldots, M_{2_m})$, and $M \triangleq M_2 - M_1$ is positive definite with diagonal entries M_{ii}, $i = 1, \ldots, m$. Next, define the set of allowable nonlinearities $\phi(\cdot)$ by

$$\Phi \triangleq \{\phi : \mathbb{R}^m \to \mathbb{R}^m : M_{1_i} u_i^2 \leq \phi_i(u)u_i \leq M_{2_i} u_i^2,$$
$$u_i \in \mathbb{R}, i = 1, \ldots, m, u \in \mathbb{R}^m\} \tag{5}$$

Next we decompose the nonlinearity $\phi(\cdot)$ into linear and nonlinear parts so that $\phi[u(t)] = \phi_s[u(t)] + M_1 u(t)$. In this case the closed-loop system (1–4) has a state space representation

$$\dot{\tilde{x}}(t) = \tilde{\tilde{A}}\tilde{x}(t) - \tilde{B}\phi_s(u), \qquad \tilde{x}(0) = \tilde{x}_0 \tag{6}$$

$$u(t) = \tilde{C}\tilde{x}(t) \tag{7}$$

where

$$\tilde{x}(t) \triangleq \begin{bmatrix} x(t) \\ x_c(t) \end{bmatrix}, \qquad \tilde{\tilde{A}} \triangleq \begin{bmatrix} A & -BM_1C_c \\ B_cC & A_c \end{bmatrix}$$

$$\tilde{B} \triangleq \begin{bmatrix} B \\ 0 \end{bmatrix}, \qquad \tilde{C} \triangleq [0 \quad C_c]$$

Note that the shifted nonlinearities $\phi_s(\cdot)$ belong to the set Φ_s given by

$$\Phi_s \triangleq \{\phi_s : \mathbb{R}^m \to \mathbb{R}^m : 0 \leq \phi_{s_i}(u)u_i \leq M_{ii}u_i^2,$$
$$u_i \in \mathbb{R}, i = 1, \ldots, m, u \in \mathbb{R}^m\} \tag{8}$$

III. Controller Design

In this section we present the main theorem characterizing fixed-order (i.e., full- and reduced-order) dynamic compensators for absolute stabilization. For the statement of this result let R_1, V_1, and R_2, V_2 be arbitrary nonnegative definite and positive definite matrices, respectively, and define the notation

$$A_\epsilon \triangleq A + \tfrac{1}{2}\epsilon I_n, \qquad \tilde{R}_0 \triangleq 2HM^{-1}$$

$$R_{2a} \triangleq R_2 + H\tilde{R}_0^{-1}H, \qquad P_a \triangleq (M_1 + H\tilde{R}_0^{-1})B^TP$$

$$\bar{\Sigma} \triangleq C^TV_2^{-1}C, \qquad A_{\hat{P}} \triangleq A_\epsilon - Q\bar{\Sigma} + B\tilde{R}_0^{-1}B^TP$$

$$A_Q \triangleq A_\epsilon + B\tilde{R}_0^{-1}B^T(P + \hat{P})$$

$$A_{\hat{Q}} \triangleq A_\epsilon + B\tilde{R}_0^{-1}B^TP - B(M_1 + \tilde{R}_0^{-1}H)R_{2a}^{-1}P_a$$

for arbitrary $P, Q, \hat{P} \in \mathbb{R}^{n\times n}$, $\epsilon > 0$, and diagonal positive definite matrix $H \in \mathbb{R}^{m\times m}$. Furthermore, define $\Phi_b \subseteq \Phi$ such that the input nonlinearity $\phi(u) \in \Phi_b$ is contained in Φ for a finite range of its argument u, that is,

$$\phi \in \Phi_b \triangleq \{\phi : \mathbb{R}^m \to \mathbb{R}^m : M_{1_i}u_i^2 \leq \phi_i(u)u_i \leq M_{2_i}u_i^2,$$
$$\underline{u}_i \leq u_i \leq \bar{u}_i, i = 1, \ldots, m\} \tag{9}$$

where $\underline{u}_i < 0$ and $\bar{u}_i > 0$, $i = 1, \ldots, m$, are given. Finally, for $i \in \{1, \ldots, m\}$, define

$$\Psi_i(\alpha) \triangleq \frac{\tilde{C}_i\tilde{A}\tilde{P}^{-1}\tilde{A}^T\tilde{C}_i^T\alpha^2}{(\tilde{C}_i\tilde{P}^{-1}\tilde{C}_i^T)(\tilde{C}_i\tilde{A}\tilde{P}^{-1}\tilde{A}^T\tilde{C}_i^T) - (\tilde{C}_i\tilde{A}\tilde{P}^{-1}\tilde{C}_i^T)^2} \tag{10}$$

$$V_i^+ \triangleq \Psi_i(\bar{u}_i), \qquad V_i^- \triangleq \Psi_i(\underline{u}_i)$$
$$V_S \triangleq \min_{i=1,\ldots,m}\{\min(V_i^+, V_i^-)\} \tag{11}$$

$$\mathcal{D}_A \triangleq \{\tilde{x} \in \mathbb{R}^{\tilde{n}} : V(\tilde{x}) < V_S, \qquad \underline{u}_i \leq \tilde{C}_i\tilde{x} \leq \bar{u}_i, \; i = 1, \ldots, m\} \tag{12}$$

where $\tilde{C}_i$ is the ith row of $\tilde{C}$, $\tilde{A} \triangleq \tilde{\tilde{A}} + \tilde{B}M_1\tilde{C}$, and $\tilde{P} \in \mathbb{R}^{\tilde{n}\times\tilde{n}}$, $\tilde{P} > 0$, satisfies

$$(\tilde{A} - \tilde{B}M_1\tilde{C})^T\tilde{P} + \tilde{P}(\tilde{A} - \tilde{B}M_1\tilde{C}) + (H\tilde{C} - \tilde{B}^T\tilde{P})^T$$
$$\times [2HM^{-1}]^{-1}(H\tilde{C} - \tilde{B}^T\tilde{P}) + \epsilon\tilde{P} + \tilde{R} = 0 \tag{13}$$

where

$$\tilde{R} \triangleq \begin{bmatrix} R_1 & 0 \\ 0 & C_c^TR_2C_c \end{bmatrix}$$

Received March 18, 1996; revision received June 27, 1996; accepted for publication June 28, 1996.

*Associate Professor, School of Aerospace Engineering.
†Adjunct Professor, School of Aerospace Engineering.

Theorem 3.1 (Ref. 3). Let $n_c \leq n$, assume $\tilde{R}_0 > 0, H > 0, \epsilon > 0$, and $\tilde{B}$ is full column rank. Furthermore, assume that there exist $n \times n$ nonnegative-definite matrices P, Q, $\hat{P}$, and $\hat{Q}$ satisfying

$$A_\epsilon^T P + P A_\epsilon + R_1 + P B \tilde{R}_0^{-1} B^T P - P_a^T R_{2a}^{-1} P_a + \tau_\perp^T P_a^T R_{2a}^{-1} P_a \tau_\perp = 0 \quad (14)$$

$$A_Q Q + Q A_Q^T + V_1 - Q\bar{\Sigma} Q + \tau_\perp Q \bar{\Sigma} Q \tau_\perp^T = 0 \quad (15)$$

$$A_{\hat{P}}^T \hat{P} + \hat{P} A_{\hat{P}} + \hat{P} B \tilde{R}_0^{-1} B^T \hat{P} + P_a^T R_{2a}^{-1} P_a - \tau_\perp^T P_a^T R_{2a}^{-1} P_a \tau_\perp = 0 \quad (16)$$

$$A_{\hat{Q}} \hat{Q} + \hat{Q} A_{\hat{Q}}^T + Q\bar{\Sigma} Q - \tau_\perp Q \bar{\Sigma} Q \tau_\perp^T = 0 \quad (17)$$

$$\operatorname{rank}\hat{Q} = \operatorname{rank}\hat{P} = \operatorname{rank}\hat{Q}\hat{P} = n_c \quad (18)$$

$$\hat{Q}\hat{P} = G^T \hat{M} \Gamma, \qquad \Gamma G^T = I_{n_c}, \qquad \hat{M} \in \mathbb{R}^{n_c \times n_c} \quad (19)$$

$$\tau \triangleq G^T \Gamma, \qquad \tau_\perp \triangleq I_n - \tau \quad (20)$$

and let A_c, B_c, and C_c be given by

$$A_c = \Gamma\left[A - Q\bar{\Sigma} + B\tilde{R}_0^{-1} B^T P - B\left(M_1 + \tilde{R}_0^{-1} H\right) R_{2a}^{-1} P_a\right] G^T \quad (21)$$

$$B_c = \Gamma Q C^T V_2^{-1} \quad (22)$$

$$C_c = R_{2a}^{-1} P_a G^T \quad (23)$$

Furthermore, suppose $(\tilde{A}, \tilde{R})$ is observable. Then

$$\tilde{P} = \begin{bmatrix} P + \hat{P} & -\hat{P} G^T \\ -G\hat{P} & G\hat{P}G^T \end{bmatrix}$$

satisfies Eq. (13) and the closed-loop system (6), (7) is globally asymptotically stable for all $\phi(\cdot) \in \Phi$. In addition, if $\phi(\cdot) \in \Phi_b$ then the closed-loop system (6), (7) is locally asymptotically stable, and $\mathcal{D}_A$ defined by Eq. (12) is a subset of the domain of attraction of the closed-loop system.

Theorem 3.1 provides constructive sufficient conditions that yield dynamic feedback gains (A_c, B_c, C_c) for absolute stabilization. When solving Eqs. (14–17) numerically, the matrices M_1, M_2, and H appearing in the design equations can be adjusted to maximize the allowable input sector bounds. For details see Ref. 3.

Remark 3.1. A key application of Theorem 3.1 is the case in which $\phi(u)$ represents a vector of saturation nonlinearities. Specifically, let $\phi[u(t)] = \{\phi_1[u_1(t)], \ldots, \phi_m[u_m(t)]\}$, where $\phi_i[u_i(t)]$, for $i \in \{1, \ldots, m\}$, is characterized by

$$\begin{aligned} \phi_i[u_i(t)] &= u_i(t), & |u_i(t)| &\leq a_i \\ \phi_i[u_i(t)] &= a_i \operatorname{sgn}[u_i(t)], & |u_i(t)| &> a_i \end{aligned} \quad (24)$$

Then Theorem 3.1 can be used to guarantee asymptotic stability of the closed-loop system (6), (7) for all $\phi(\cdot)$ satisfying Eqs. (24) with a guaranteed domain of attraction. In particular, if $M_1 > 0$ and $M_2 = I \geq M_1 > 0$ and there exists a positive-definite matrix $\tilde{P}$ satisfying Eq. (13), then take $\bar{u}_i = -\underline{u}_i = a_i/M_{1_i}, i = 1, \ldots, m$, in Eq. (12).

IV. Homotopy Algorithm

In this section we present a numerical algorithm for solving the design equations given by Theorem 3.1. This algorithm is similar to the continuation algorithm presented in Ref. 4.

Algorithm 4.1. To solve the design equations (14–17), carry out the following steps.

Step 1. Initialize $j = 0$ and $\tau = I_n$. Select $j_{\max}$ and H.

Step 2. Solve Eqs. (14–17) for P, Q, $\hat{P}$, and $\hat{Q}$.

2a. Solve Eq. (14) for P.

2b. For an initial guess of Q solve Eq. (16) for $\hat{P}$. Update Q by solving Eq. (15) with the current values of P and $\hat{P}$.

2c. Compute the residual error in Eqs. (15) and (16). If the norm of the residual error in the Q and $\hat{P}$ equations satisfies some preassigned tolerance, then go to Step 2d. Else go to Step 2b.

2d. Solve Eq. (17) for $\hat{Q}$.

Step 3. To update τ, form the contragradient diagonalization of $\hat{Q}$ and $\hat{P}$ and use the procedure outlined in Ref. 4.

Step 4. If $j = j_{\max}$ or $[\operatorname{tr}(\tau) - n_c]/n_c$ is less than some preassigned tolerance, then go to Step 5. Else let $j = j + 1$ and go to Step 2.

Step 5. Compute the Γ, G^T factorizations of τ using the contragradient diagonalization transformation obtained in Step 3. See Ref. 4 for details.

Step 6. Compute A_c, B_c, and C_c using Eqs. (21–23).

V. Illustrative Numerical Examples

Example 5.1. Our first example considers full-order controllers for a single-input/single-output F-16 fighter aircraft with an elevator deflection amplitude constraint.[5] Specifically, we consider the linearized pitch axis longitudinal dynamics model of an F-16 fighter aircraft at nominal flight conditions (3000 ft and Mach number of 0.6) given by

$$\dot{x}(t) = \begin{bmatrix} 0 & 1 & 0 \\ 0 & -0.87 & 43.22 \\ 0 & 0.99 & -1.34 \end{bmatrix} x(t) - \begin{bmatrix} 0 \\ -17.25 \\ -0.17 \end{bmatrix} \phi[u(t)] \quad (25)$$

$$y(t) = [1 \quad 0 \quad 0] x(t) \quad (26)$$

where

$$x = \begin{bmatrix} \theta\text{: pitch attitude} \\ q\text{: pitch rate} \\ \alpha\text{: angle of attack} \end{bmatrix}$$

$$y = \theta, \qquad u = \delta_e\text{: elevator deflection}$$

The elevator deflection amplitude constraint $\phi[u(t)]$ is characterized by Eq. (24) with $i = 1$ and $a_1 = 0.6$. Choosing the design parameters $V_1 = I_3$, $V_2 = 1$, $R_1 = \operatorname{diag}[2500, 1, 1]$, $R_2 = 100$, $M_1 = 0.2$, $M_2 = 1.0$, and $H = 1809$, a full-order dynamic controller ($n_c = 3$) was designed using Theorem 3.1 with guaranteed domain of attraction $\mathcal{D}_A = \{\tilde{x} : \tilde{x}^T \tilde{P} \tilde{x} < 2.313 \times 10^2, |\tilde{C}\tilde{x}| \leq 0.6\}$. To illustrate the closed-loop behavior of the system, let $x_0 = [0.1 \ 0 \ 0]^T$ and $x_{c_0} = 0_{3\times 1}$. Note that $\tilde{x}_0^T \tilde{P} \tilde{x}_0 = 1.088 \times 10^4$, so that $\tilde{x}_0 \notin \mathcal{D}_A$. However, it can be seen from Fig. 1a that the controller designed using Theorem 3.1 results in an asymptotically stable system with satisfactory performance, whereas the linear quadratic Gaussion (LQG) controller in the presence of an input saturation nonlinearity results in an unstable system. Finally, Fig. 1b provides a comparison of $\phi[u(t)]$ for the three designs.

Example 5.2. This example is adopted from Ref. 3 and involves four coupled rotating disks. The control objective is to control the angular displacement of the first disk using a torque input at the location of the third disk. The plant is of the eighth order and has a rigid body mode. The problem data are given in Ref. 3. Here we assume that the control torque amplitude is limited so that $\phi[u(t)]$ is characterized by Eq. (24) with $i = 1$ and $a_1 = 4$. Choosing the design variables $M_1 = 0.1$, $M_2 = 1$, and $H = 1.0561$, a second-order ($n_c = 2$) dynamic compensator was designed using Theorem 3.1 with guaranteed domain of attraction $\mathcal{D}_A = \{\tilde{x} : \tilde{x}^T \tilde{P} \tilde{x} < 897.4248, |\tilde{C}\tilde{x}| \leq 4\}$. To illustrate the closed-loop behavior, let $x_0 = [-2 \ 1 \ 3 \ 4 \ 0 \ 1 \ 3 \ 1]^T$ and $x_{c_0} = 0_{2\times 1}$. Note that $\tilde{x}_0^T \tilde{P} \tilde{x}_0 = 26.2481$ and $\tilde{C}\tilde{x}_0 = 0$ and hence $\tilde{x}_0 \in \mathcal{D}_A$. The closed-loop behavior with the reduced-order controller in the presence of input saturation is shown in Fig. 2. Note that a second-order balanced truncated LQG controller destabilizes the nominal and saturated system.

Example 5.3. Consider the asymptotically stable system

$$\dot{x}(t) = \begin{bmatrix} -0.2 & 1 & 0 \\ 0 & -0.2 & 1 \\ 0 & 0 & -0.2 \end{bmatrix} x(t) - \begin{bmatrix} 0 \\ 0 \\ 1 \end{bmatrix} \phi[u(t)] \quad (27)$$

$$y(t) = [1 \quad 0 \quad 0] x(t) \quad (28)$$

where the saturation nonlinearity $\phi[u(t)]$ is given by Eq. (24) with $i = 1$ and $a_1 = 1$. Choosing the design parameters $R_1 = I_3$, $R_2 = 100$,

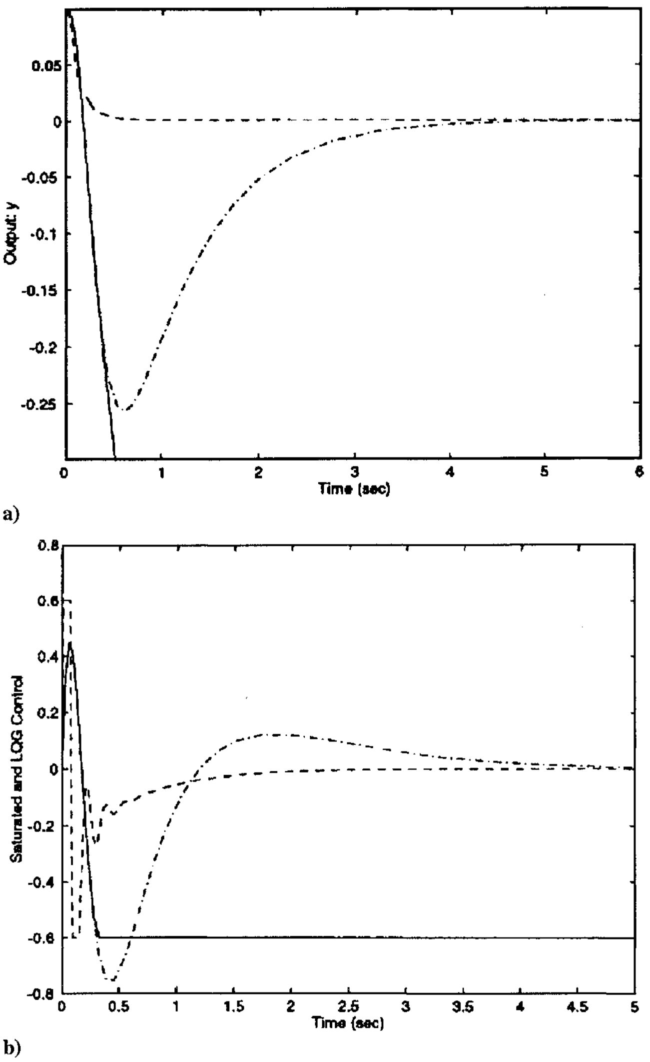

Fig. 1 LQG, ---; saturated LQG, ——; and Theorem 3.1, – – –, designs.

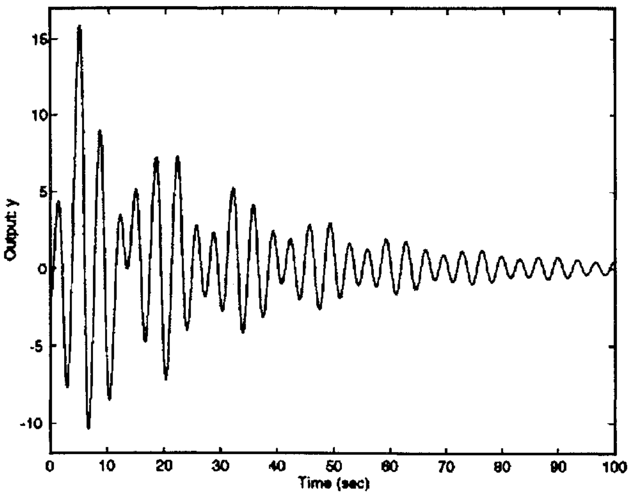

Fig. 2 Reduced-order saturation controller.

$V_1 = I_3$, $V_2 = 1$, $M_1 = 0.1$, $M_2 = 1.0$, and $H = 8348$, a second-order ($n_c = 2$) dynamic compensator was designed using Theorem 3.1 with guaranteed domain of attraction $\mathcal{D}_A = \{\tilde{x}:\tilde{x}^T\tilde{P}\tilde{x} < 2.7137 \times 10^5, |\tilde{C}\tilde{x}| \leq 1\}$. Furthermore, with the given weighting matrices an LQG controller was designed that was model reduced to obtain a second-order controller. To illustrate the closed-loop behavior of the system, let $x_0 = [-40 \quad -25 \quad 30]^T$ and $x_{c_0} = 0_{2\times 1}$. Note that $\tilde{x}_0^T\tilde{P}\tilde{x}_0 = 4.0673 \times 10^5$ so that $\tilde{x}_0 \notin \mathcal{D}_A$. Figure 3a shows

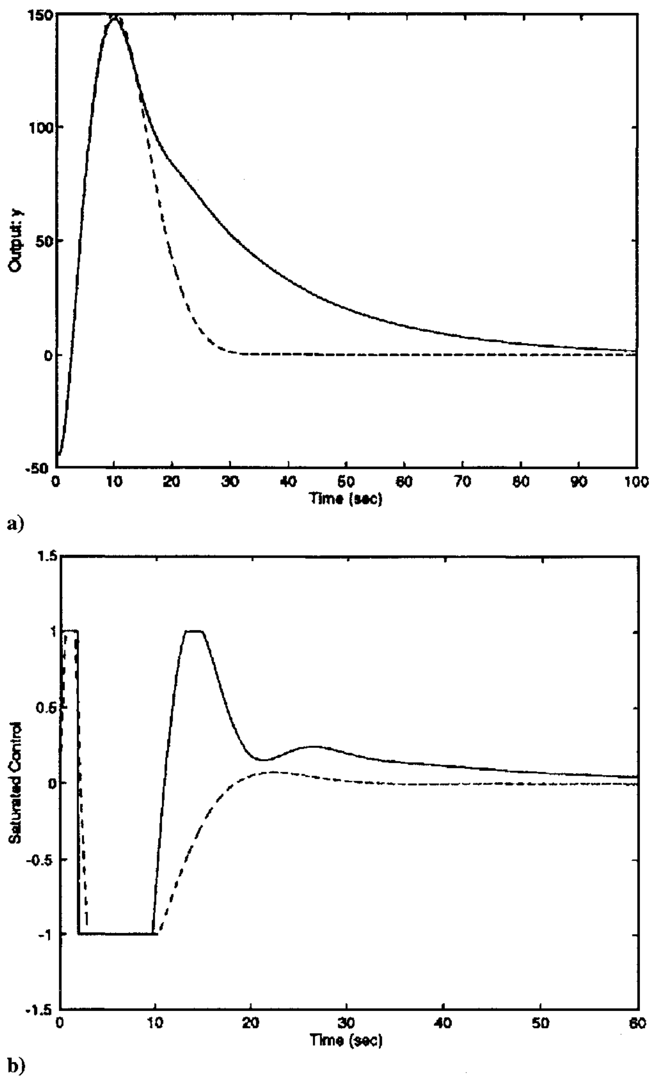

Fig. 3 Designs: ——, model-reduced LQG and – – –, Theorem 3.1.

the closed-loop behavior for the controller designed using Theorem 3.1 and the model-reduced LQG controller. Finally, Fig. 3b provides a comparison of $\phi[u(t)]$ for the two designs.

VI. Conclusion

In this Note we designed antiwindup controllers. A numerical algorithm based on a continuation algorithm was developed for solving the nonlinear design equations characterizing full- and reduced-order dynamic compensators. A series of design studies was presented to demonstrate the effectiveness of the approach.

Acknowledgments

This research was supported in part by the National Science Foundation under Grant ECS-9496249 and the U.S. Air Force Office of Scientific Research under Grant F49620-96-1-0125.

References

[1]Bernstein, D. S., and Haddad, W. M., "Nonlinear Controllers for Positive Real Systems with Arbitrary Input Nonlinearities," *IEEE Transactions on Automatic Control*, Vol. AC-39, No. 7, 1994, pp. 1513–1517.

[2]Anon., "Special Issue on Saturating Actuators," *International Journal of Robust and Nonlinear Control*, Vol. 5, 1995.

[3]Haddad, W. M., and Kapila, V., "Fixed-Architecture Controller Synthesis for Systems with Input-Output Time-Varying Nonlinearities," *Proceedings of the American Control Conference* (Seattle, WA), Inst. of Electrical and Electronics Engineers, Piscataway, NJ, 1995, pp. 4396–4400; also *International Journal of Robust and Nonlinear Control* (to be published).

[4]Greeley, S. W., and Hyland, D. C., "Reduced-Order Compensation: Linear-Quadratic Reduction Versus Optimal Projection," *Journal of Guidance, Control, and Dynamics*, Vol. 11, No. 4, 1988, pp. 328–335.

[5]Schmitendorf, W. E., "Stabilization via Dynamic Output Feedback: A Numerical Approach," *Journal of Guidance, Control, and Dynamics*, Vol. 14, No. 5, 1991, pp. 1083–1086.

Explicit Guidance for Aeroassisted Orbital Plane Change

Der-Ming Ma*
Tamkang University,
Tamsui, Taiwan 25137, Republic of China

Introduction

OVER the past several years, considerable research has been done on both coplanar and noncoplanar aeroassisted orbital transfer.[1] For noncoplanar orbital transfer, the guidance schemes based on the optimal trajectories have been of particular interest.[2] For re-entry lifting vehicles, it has been shown that there are two different kinds of control strategy for optimal plane change.[3,4] In the first control strategy, the vehicle initially pulls down to the denser atmosphere but, before the minimum altitude is reached, the vehicle pulls up to leave the atmosphere. In the second strategy, the vehicle initially pulls up to avoid entering too deeply into the denser atmosphere. Once the minimum altitude is reached, the pullup level decreases and the vehicle leaves the atmosphere. It may be argued that, for the first kind of maneuver, the vehicle has a slightly shallow entry angle, and the control is used to overcome the tendency of pulling up. For the second kind of maneuver, the vehicle enters the atmosphere with a slightly larger entry angle. Because there is a natural tendency to pull up, a slightly smaller control then is needed to pull up the vehicle. This overview suggests the problem of finding an optimal entry angle, so that the vehicle does not need to pull down or pull up for the given plane change. This note presents an explicit guidance law of a re-entry aeroassisted orbital vehicle. The vehicle enters the atmosphere with a prescribed entry angle and keeps the bank angle at 90 deg until exit. The entry angle is a function of the entry speed and the exit speed. The lift control in the atmosphere can be divided into two phases. In the first phase, the vehicle descends and keeps the normalized lift coefficient constant. During ascent, the normalized lift coefficient decreases proportionally to the increase in height. A comparison is made for the orbital plane change between the optimal aeroassisted trajectory and the trajectory realized by the explicit guidance. The proposed guidance scheme is simple to implement and produces nearly optimal plane change.

Dimensionless Equations of Motion

The motion of the re-entry vehicle over a spherical nonrotating planet is defined by the six variables, r (radius), θ (longitude), ϕ (latitude), V (velocity), γ (flight-path angle), and ψ (heading).[5]

Using a parabolic drag polar of the form, $C_D = C_{D_0} + KC_L^2$, we define the normalized lift coefficient $\lambda = C_L/C_L^*$, where C_L^* is the lift coefficient corresponding to the maximum lift-to-drag ratio E^*. The atmosphere is assumed to be at rest with respect to the planet and with a locally exponential property, $\rho = \rho_0 e^{-\beta(r-r_0)}$. The gravitational force field is given by the usual inverse-square force law. Without loss of generality, we can use the equatorial plane as the reference plane. We introduce the dimensionless variables $u = V^2/g_0 r_0$ and $h = (r - r_0)/r_0$ to represent speed and range, respectively, and define the dimensionless arc length as

$$s = \int_0^t \frac{V}{r}\cos\gamma\,\mathrm{d}t \tag{1}$$

to replace time as the independent variable. The coefficient B, which specifies the starting flight altitude, is given by

$$B = \frac{\rho_0 S C_L^* r_0}{2m} \tag{2}$$

where S is the reference area. The dimensionless equations of motion, with the bank angle $\sigma = 90$ deg, are

$$\frac{\mathrm{d}h}{\mathrm{d}s} = (1+h)\tan\gamma \tag{3a}$$

$$\frac{\mathrm{d}\theta}{\mathrm{d}s} = \frac{\cos\psi}{\cos\phi} \tag{3b}$$

$$\frac{\mathrm{d}\phi}{\mathrm{d}s} = \sin\psi \tag{3c}$$

$$\frac{\mathrm{d}\psi}{\mathrm{d}s} = \frac{B\lambda(1+h)e^{-h/\varepsilon}}{\cos^2\gamma} - \cos\psi\tan\phi \tag{3d}$$

$$\frac{\mathrm{d}u}{\mathrm{d}s} = -\frac{B(1+h)u(1+\lambda^2)e^{-h/\varepsilon}}{E^*\cos\gamma} - \frac{2}{1+h}\tan\gamma \tag{3e}$$

$$\frac{\mathrm{d}\gamma}{\mathrm{d}s} = 1 - \frac{1}{u(1+h)} \tag{3f}$$

Note that $\varepsilon = 1/\beta r_0$, which characterizes the atmosphere. In these dimensionless equations, the only physical characteristics to be specified are the vehicle's maximum lift-to-drag ratio and the coefficient B. In this problem, the choice of $B = 0.006$ specifies the initial entry altitude and is in the region suggested by Vinh et al.[6]

In the problem of optimal plane change, the initial values of states are

$$h_0 = 0, \quad \theta_0 = 0, \quad \phi_0 = 0, \quad \psi_0 = 0$$
$$u_0 = \text{given}, \quad \gamma_0 = \text{free} \tag{4a}$$

and the final values are

$$h_f = \text{free}, \quad \theta_f = \text{free}, \quad \phi_f = \text{free}$$
$$\psi_f = \text{free}, \quad u_f = \text{given}, \quad \gamma_f = \text{free} \tag{4b}$$

Note that in this problem the lift is the only control.

Variational Formulation

Because the plane change I_f is going to be maximized, we have the following cost function J to be minimized:

$$J = \cos I_f = \cos\phi_f\cos\psi_f \tag{5}$$

Using the maximum principle, we introduce the adjoint variables p_x to form the Hamiltonian

$$H = p_h(1+h)\tan\gamma + p_\theta\frac{\cos\psi}{\cos\phi} + p_\phi\sin\psi + p_\psi\left[\frac{B\lambda(1+h)e^{-h/\varepsilon}}{\cos^2\gamma} - \cos\psi\tan\phi\right] - p_u\left[\frac{B(1+h)u(1+\lambda^2)e^{-h/\varepsilon}}{E^*\cos\gamma} + \frac{2}{1+h}\tan\gamma\right] + p_\gamma\left[1 - \frac{1}{u(1+h)}\right] \tag{6}$$

Presented as Paper 94-3527 at the AIAA Atmospheric Flight Mechanics Conference, Scottsdale, AZ, Aug. 1–3, 1994; received June 15, 1995; revision received June 14, 1996; accepted for publication June 15, 1996.

*Associate Professor, Department of Aerospace Engineering. Member AIAA.